Artificial Neural Network for performance prediction of Absorption Chillers of Large-Scale Solar-Air-Conditioning Systems.

Lukas Feierl[1], Peter Innerhofer[1], Hannes Poier[1], Maria Moser[1] and Christian Holter[1]

[1] SOLID GmbH, Graz (Austria)

Abstract

As environmentally-friendly alternative to vapor compression chiller, solar-driven absorption machines can be used to satisfy cooling demand. To improve confidence in this technology, good simulation and monitoring tools are needed to ensure the optimal performance of the systems. However, the performance prediction of absorption chiller is no easy task if non-steady states and good accuracy are required. As proposed by various authors, artificial neural networks (ANN) proved useful for providing easy to implement, yet very accurate ways of predicting the performance of absorption machines. Hence, this paper aims to further explore the limits of these ANN performance predictions, this paper attempts to apply the model to four of the currently largest solar thermal air-conditioning (SAC) plants. The results show, that the ANN works very well on all the solar systems with R^2 of 95% and RMSE of lower than 2.3°C, 0.8°C and 0.4°C for the hot water, cooling water and chiller water side respectively. Furthermore, the results indicate that the ANN can even be used for fault detection and for analysation purposes.

Keywords: solar cooling; large-scale; absorption chiller; performance prediction; artificial neural network;

1. Introduction

The energy demand for cooling is rising rapidly in the recent years due to population and economic growth (OECD/IEA 2018). At the present time, this cooling demand is satisfied almost entirely by the use of electric-driven vapor compression chillers. However, there are some drawbacks of using these types of air conditioning systems (ACs): Firstly, if the temperature rises above a certain level such that all ACs in the area start almost simultaneously, this results in very high electric peak loads. This behavior is quite complicated to handle for the electric grids. Secondly, the cooling is only provided locally, but there is also waste heat produced that is transferred to the surroundings, creating even more cooling demand for adjacent buildings. If a lot of vapor-compression chiller are used in the same area, this can lead to the so-called “urban heat islands” effect as pointed out by Lazrak et al. (2016) and Pons et al. (2012).

As an alternative, solar air-conditioning systems (SACs) can be used to provide renewable and environmentally-friendly energy, by powering an absorption chiller with solar thermal heat. Conveniently, solar power is always available when cooling demand is high due to the relation of solar irradiation and high ambient temperatures, increasing the potential of the technology even further. Furthermore, besides solar cooling a variety of different applications can become important in diverse future energy systems. Flue gas condensation (HPT TCP, 2018a) and system combinations with seasonal heat storages (HPT TCP, 2018b) are two examples. However, to increase the market share and to improve the trust and confidence in this technology, good simulation models and monitoring tools are needed to ensure the optimal performance of SAC systems.

For absorption machines a variety of performance prediction models already exist, each varying in complexity, accuracy and validity conditions. While most models are either very complex to implement, not applicable to dynamic operating conditions or derived for specific chiller types only, artificial neural networks (ANN) were shown to be useful for modelling chillers at non-steady state conditions while being very accurate and easy to implement (Nasruddin et al. 2019; Xu and Wang 2017; Lazrak et al. 2016; Frey et al. 2014; Rosiek and Batlles 2011, 2010; Manohar et al. 2006). However, until now, studies either focused on rather small absorption machines or were conducted with steady-state data only. To further explore the limits of the ANN-performance prediction, this paper attempts to apply the neural network model to four of the currently largest solar thermal air-conditioning plants, covering different system-layouts and climate conditions. This way, the ANN can be tested on the absorption machines of large-scale systems in operation and individual results for each system can be analyzed and compared.

doi:10.18086/swc.2019.03.01 Available at http://proceedings.ises.org

2. Method

2.1 Introduction to Artificial Neural Networks

Basically, an artificial neural network (ANN) is a mathematical function with adjustable weights. The name of ANNs derived from its resemblance to the processing of information in the brain (see Fig.1). For example, in pattern recognition an image (the input) is handled by a network of neurons where each of the neurons processes the information that is received from previous ones. The result is then sent to the next layer of neurons and so on, until finally some output (e.g. the classification of the image) is generated. Similarly, the ANN consists of layers of non-linear functions (the neural nodes) that are connected to one another by weighed connections. Therefore, the nodes resemble the action of the neurons on the input. On the other hand, the weights act similar as the neuro-transmitter between the dendrite and the synaptic terminals, which amplify or damp the signals from the other neurons.

The choice of function that is used at the output nodes is dependent of the type of the problem. In the case of continuous output values[1] linear functions are sufficient, as they allow to calculate continuous values and have other useful properties. The functions on the hidden layers, however, have to be non-linear. This is important as it enables the network to model a wider range of problems which one could not mimic with linear functions alone. The specific choice of function is arbitrary, but usually logistic, sigmoid or tanh functions are chosen, due to their useful properties related to their derivation (Bishop 2006).

In summary, an artificial neural network transforms some input to some output values, where the output values are highly dependent on the weights. Moreover, it has even been proven that ANNs are *universal approximators*, meaning that they are able to mimic any kind of continuous function as long as the weights are adjusted correctly (Bishop 2006) [2].

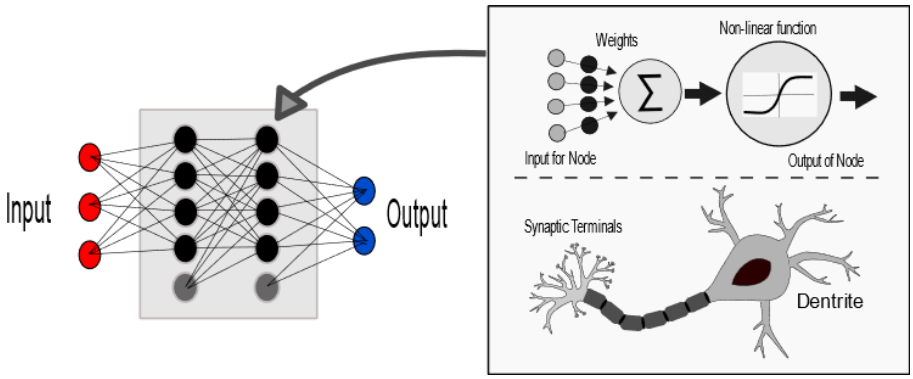

Fig. 1: Sketch of a neural network with input nodes in red, output nodes in blue and two hidden layers in gray. The weighs are displayed as black lines. On the right side of the figure, the similarity between neural nodes and neurons is visualized schematically.

This adjustment of weights can be done by supervised learning, that is, by supplying some training data with known output to a specific ANN-model and altering the weights until the predicted values match the output from the training set. The detailed process of calculating the weights based on the data is usually done by *Backpropagation* and is described in (Bishop, 2006). However, as most of the needed algorithms have already been implemented in various programming languages, the creation of neural networks has become rather easy. This, combined with the fact that ANNs allow to model arbitrary functions without much information about the underlying processes, has made artificial neural networks very popular in the field of machine learning.

2.2 Absorption Chiller model

For the proposed task of modelling absorption chiller via ANNs, various authors have shown that rather simple architectures are sufficient for the performance prediction. In accordance to Lazrak et al. (2016) and Frey et al. (2014) the volume flow $\dot{\boldsymbol{m}}$ and the input temperatures of the chiller $\boldsymbol{T_{in}}$ have been chosen as input values, while the outlet temperatures of the chiller are used as the output. Hence, the function that the neural network should mimic is given by:

$$\mathbf{T_{out}} \cong f_{ANN}\,(\mathbf{T},\ \dot{\boldsymbol{m}}) \qquad \text{(eq.1)}$$

[1] In contrast to classification problems where the output are True/False or probabilistic values.

[2] This holds true as long as (1) the output of the function to be predicted depends solely on the known input, (2) there is enough data available for training and (3) the architecture for the ANN is complex enough (i.e. the used functions and the number of nodes and layers are chosen well).

with the abbreviations:

$$\dot{\boldsymbol{m}} = (\dot{m}_{Hot\ inlet},\ \dot{m}_{Recooling\ inlet},\ \dot{m}_{Cold\ inlet}) \quad \text{(eq.2)}$$

$$\mathbf{T} = (T_{Hot\ inlet},\ T_{Recooling\ inlet},\ T_{Cold\ inlet}) \quad \text{(eq.3)}$$

$$\mathbf{T_{out}} = (T_{Hot\ outlet},\ T_{Recooling\ outlet},\ T_{Cold\ outlet}) \quad \text{(eq.4)}$$

The resulting prediction $\mathbf{T_{out}}$ of (eq.1) then allows to calculate various performance indicators of the chiller like for example the Coefficient of Performance (COP) or Energy Efficiency Ratios (EER) by only using input data for the calculation.

As proposed by Lazrak et al. (2016), there might be a time delay such that also previous timestamps influence the resulting output temperature, especially if non-steady state conditions are considered. This can be compensated in the ANN-model by also providing the values from previous timestamps. However, in contrast to Lazrak et al. only input values are used for the computation, but not the output values of previous timesteps. Equation (eq.1) is hence modified to:

$$\mathbf{T_{out}}(\mathrm{t}) \cong f_{ANN}\begin{pmatrix}\mathbf{T}(t),\ \dots,\ \mathbf{T}(t-n\,\Delta t),\\ \dot{\boldsymbol{m}}(t),\ \dots,\ \dot{\boldsymbol{m}}(t-n\,\Delta t)\end{pmatrix} \quad \text{(eq.5)}$$

where t indicates some timestep, Δt is the monitoring interval and $n \cdot \Delta t$ is the maximal time delay to be considered. As additional feature, also the ambient temperature is introduced as input parameter, as it might influence the operation of the chiller due to heat losses.

$$\mathbf{T_{out}}(\mathrm{t}) \cong f_{ANN}\begin{pmatrix}\mathbf{T}(t),\ \dots,\ \mathbf{T}(t-n\,\Delta t),\\ \dot{\boldsymbol{m}}(t),\ \dots,\ \dot{\boldsymbol{m}}(t-n\,\Delta t),\\ T_{amb}(t),\dots,T_{amb}(t-n\Delta t)\end{pmatrix} \quad \text{where} \quad \dot{\boldsymbol{m}}(t) \neq 0 \quad \text{(eq.6)}$$

The $\dot{\boldsymbol{m}}(t) \neq 0$ is needed because the prediction is only relevant if the chiller is in operation during the current timestep t. Else, the cooldown of the temperatures in the pipes would be trained by the ANN, too. Even though it would be possible for the network to mimic the cooldown simultaneously to the in-operation case, the results are uninteresting as the equations for heat losses in pipes are known anyways. Plus, the accuracy of the cooldown-prediction would blur the results of the in-operation performance evaluation. Hence, the data is filtered such that for every predicted temperature-set $\mathbf{T_{out}}(\mathrm{t})$ the mass flows $\dot{\boldsymbol{m}}(t)$ of each circuit is higher than zero, while still allowing not-in-operation data in the previous timestamps $(t - i\Delta t)$ for $i \neq 0$.

The specific choice for the architecture of the artificial neural network is based on the works of Nasruddin et al. (2019), Xu and Wang (2017), Lazrak et al. (2016) and Frey et al. (2014). All of them show good results for the predictions by only using one to two hidden layers with 5 to 20 nodes and logistic activation functions, combined with linear functions for the output. However, to choose the best values for the ANN, the number of nodes and the time-delay are varied successively until good results are obtained within the validation.

2.3 Validation Methods

To validate the results of supervised machine learning methods, the available data is usually split into multiple parts: First, there is a training set that is used for the training of the network and the calculation of the weights. Next, there is a validation set in order to check how well the trained model can adapt to unseen data. This is important to prevent overfitting, where the ANN learns patterns that are only valid on the training data but do not apply on new data. Hence, with the validation set the parameters are optimized until both the training set and the validation set can be modelled well. Finally, a third set of the data is used for performance measurement only. It is important that the test set does not influence the training or validation in any way as this is crucial to ensure that the performance results are indeed valid for unseen data.

Usually, the sets are randomly sampled from the available data. In contrast to many machine learning problems, however, the samples of subsequent timesteps are not independent of each other as they contain information about the previous input variables (see eq.6). Hence, choosing randomly sampled values for the test set would violate the rule that the test set should be independent of the training and validation. As a result, the most recent part of the available data is chosen for the test set. The remaining previous data is randomly sampled to generate the training and the validation set., all samples corresponding to one date are always assigned to either the training or the validation set in blocks to also guarantee independence of the training and validation set (see Fig.2).

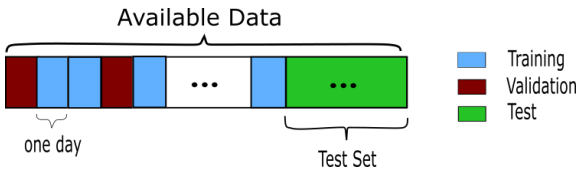

Fig. 2: Sketch visualizing the sampling of the available data. Blocks of one day minimum are assigned to either set.

For benchmarking, the following scores are used to analyze the results: First, the R²-score describes how much of the variance of the data can be described by the model. It indicates whether the chosen model is sufficient for the problem where a score of 1.0 means that the model can predict the values perfectly and 0.0 means that the prediction is very bad. With the output value to be predicted donated by y_i, the prediction of the ANN donated as $f(x_i)$, the input as x_i and the mean of the observed data $\bar{y}$, the formula for the R^2-score is given by:

$$R^2 = 1 - \frac{\sum_{i=1}^{n}(y_i - \bar{y})}{\sum_{i=1}^{n}(y_i - f(x_i))^2} \quad \text{(eq.7)}$$

Furthermore, the root mean squared error (RMSE) is used for the performance test to give a clearer understanding of how much the predicted values differ from the measured ones in terms of the specific units of the variables. It is calculated for each output variable separately and is given by:

$$RMSE = \sqrt{\frac{1}{n} \cdot \sum_{i=1}^{n}(f(x_i) - y_i)^2} \quad \text{(eq.8)}$$

3. Data Selection

For the training, validation and testing of the ANN-model that is proposed in section 2, the data of four large-scale solar-air conditioning systems is used. All selected systems were built and are operated by the solar thermal specialist SOLID. With cooling capacities of approximately 1MW they belong to the currently largest solar thermal air-conditioning systems (Weiss and Spörk-Dür 2018) and thus have been studied previously by various authors (Feierl et al. 2018; Olsacher and Schnitzer 2016; Schubert et al. 2014, 2011; Buchinger et al. 2012). An overview of the characteristics of the selected systems can be seen in Tab.1.

The systems are closely monitored by the Methodiqa-Software (Ohnewein et al. 2015) which provides pre-processed data with a 5-Minute time interval. Before applied to the ANN, each input and output variable gets normalized so that its values range from minus one to one. This is important as the logistic activation functions used for the hidden layer work best within this domain. The chosen minimum and maximum values for each system and respective temperature and mass-flow rates can be seen in Tab.2. The initialisation, training and validation of the neural networks was done with Python while strongly relying on the scikit-learn library (Pedregosa et al., 2011) for designing and managing the neural network.

Tab. 1: Overview of characteristics of the selected solar thermal air-conditioning systems.

Name	Location	Time of commission	Collector area	Cooling capacity	Type	Chiller
United World College	Singapore	2011	3872 m²	1477 kW	Domestic Hot Water and Cooling	BROAD BDH127X
Desert Mountain High School	Arizona	2014	4935 m²	1750 kW	Cooling	BROAD BDH151X
Hospital Managua	Nicaragua	2017	4450 m²	1023 kW	Domestic Hot Water and Cooling	Carrier 16 JL R024
Ikea Alexandra	Singapore	2017	2472 m²	880 kW	Cooling	BROAD BDHY76X

Tab.2: Temperature and volume flow ranges at each system during operation.

Section	Variable	UWC	DMHS	Managua	Ikea
Hot water	Inlet Temperature [°C]	50 – 100	45 – 115	45 – 110	40 – 110

	Outlet temperature [C]	40 – 90	40 – 105	45 – 105	40 – 90
	Volume Flow [m³/h]	88 – 100	78 – 117	25 – 119	30 – 115
Cooling water	Inlet Temperature [°C]	23 – 30	20 – 45	22 – 30	25 – 32
	Outlet temperature [C]	24 – 34	18 – 40	25 – 45	27 – 38
	Volume Flow [m³/h]	510	218 - 436	166 – 276	160 - 245
Chilled Water	Inlet Temperature [°C]	6 – 20	5 – 30	8 – 20	11 – 18
	Outlet temperature [C]	4 – 16	3 – 25	5 – 15	8 – 16
	Volume Flow [m³/h]	79 – 84	90 – 243	88 – 126	66 – 165
Ambient	Temperature [°C]	24 – 36	5 – 45	20 – 45	24 – 45

3.1 United World College (UWC)

The solar air conditioning system at the United World College Tampines in Singapore was commissioned by SOLID in 2011. Located in the tropical rainforest climate of Singapore with high ambient temperatures of approximately 20°C to 36°C and high humidity of approximately 80% throughout the year, the solar air-conditioning system is used to both cool the buildings using a solar powered 1475kW lithium bromide absorption chiller and furthermore providing domestic hot water for the college. For efficient energy management two 30m³ heat storages are installed between the collectors and the chiller, allowing to generate chilled water even if no radiation is available at that time. Due to being the largest solar thermal air conditioning system until 2014 it was previously studied by Olsacher and Schnitzer (2016) focusing on the financial aspects, and Schubert et al (2011) and Feierl et al. (2018) dealing with operation and performance results.

3.2 Desert Mountain High School (DMHS)

Installed in February 2014, the system at the Desert Mountain High School in Arizona is currently the largest solar thermal air conditioning system worldwide. It uses 4935m² of solar collectors to power a 1750kW lithium bromide absorption chiller that is operated in combination with 3 conventional vapor-compression chillers to cool 55000m² of air-conditioned space (Schubert et al, 2014; Olsacher and Schnitzer, 2016). Furthermore a 34.5m³ heat storage is installed to buffer the solar load. The system is located in the arid desert climate with ambient temperature ranging from 0°C up to 45°C in the summer and with varying humidity of 20% to 45% (Feierl et al. 2018).

3.3 Hospital Managua (Managua)

The third selected system is located at the Hospital *Militar Escuele Dr "Alejandro Dávila Bolaños"* in Managua, Nicaragua and was installed in 2017. The heat produced by the 4450m² flat plate solar collectors are used to provide hot water for the laundry and the hospital itself and to power a 1023kW lithium absorption chiller for cooling the building (SOLID 2019). There is a 75m³ storage installed providing the chiller with temperatures of approximately 100°C depending on the produced solar heat. The system is located in the tropical wet and dry climate, with constantly high temperatures but varying seasons featuring both heavy rainfalls and dry periods (Feierl et al., 2018).

3.4 Ikea Alexandra (Ikea)

In December 2017, a solar cooling system with 2472 m² of solar collectors were commissioned at Ikea Alexandra in Singapore (SOLID, 2019; Feierl et al., 2018). The solar heat is used for powering an 880kW absorption chiller cooling the warehouse. The demand is determined mostly by the number of visitors and thus the opening hours of the building. Similar to the other selected systems a 15m³ heatstorage is used for buffering. The system is located in Singapore's tropical rainforest climate as described previously for UWC.

4. Results

4.1 Architecture optimization

In accordance to the discussion in section 2, the described ANN-model (eq.6) is used to predict the output temperatures of the chillers at each system. In order to choose appropriate parameters for the final artificial neuronal network, multiple networks with different settings for the time delay and the number of nodes are trained and validated using the validation set. As the training and validation sets are randomly sampled at each run, each setup

is evaluated at least ten times and average values are calculated to minimize the effect of random fluctuations. The results are displayed in Fig.3.

It can be seen that both the number of nodes and the amount of time delay improves the R^2-score of the ANNs, seemingly converging to a maximal value for high numbers. The obtained scores of all systems reach up to 93% (UWC) to 96% (DMHS) indicating acceptable to very good agreement to the measured data. Furthermore, for a number of neurons higher than 25 and time-delays of more than 8 (i.e. 40min) the results are practically identical. Thus, a (8·7, 25, 3) architecture with 65 input values, 25 nodes in the hidden layer and 3 output parameters can be used for the performance evaluation in the following section.

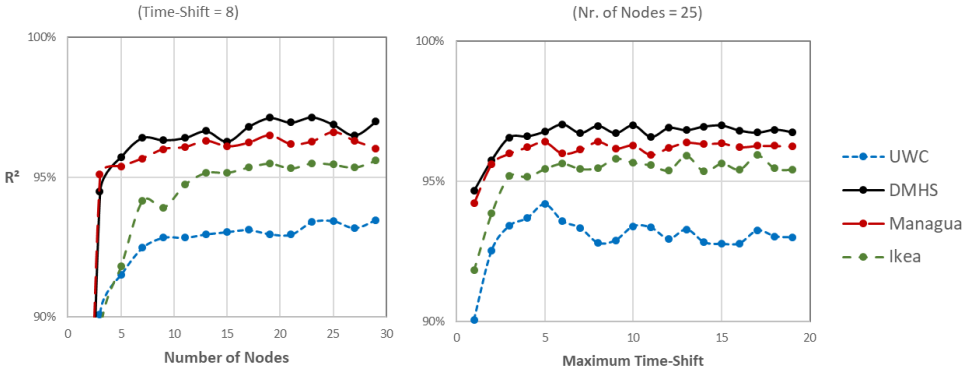

Fig. 3: Average R^2 scores for each solar system in relation to the number of nodes (left) and to the number of time shifts (right). The other parameters are held constant during these tests.

4.2 Quality of the Prediction.

Next it is evaluated how well the ANN can predict the output temperatures of the chiller at each system individually. With the derived (65, 25, 3) architecture from section 4.1, four neural networks are created and trained with the respective data of each system. In order to analyze the prediction performance, the test sets are used to compute the scores (eq7.) and (eq.8). The results for the scores for each system can be seen in Tab.3.

Tab.3 Prediction results for each individual system.

	R-squared [-]	RMSE Hot Water Temperature [°C]	RMSE Cooling Water Temperature [°C]	RMSE Chilled Water Temperature [°C]
UWC	94.45%	0.63	0.07	0.38
DMHS	90.81%	8.75	0.80	2.14
Managua	90.98%	2.29	0.38	0.41
Ikea	95.78 %	1.84	0.21	0.10
DMHS (pre-service)	97.00 %	1.49	0.26	0.27
DMHS (post-service)	87.77 %	13.26	1.12	2.92

To give a better understanding of the prediction accuracy, a comparison of measured and predicted temperatures are displayed in Fig.4. For each predicted value, the corresponding measured value is plotted on the y-axis. Hence, perfectly predicted samples would span the diagonal. A margin-line indicates errors of higher than 1°C (dashed line) and 2°C (solid line) respectively. The percentage on the upper left and the lower right show how much percent of the data is outside of the 2°C margin-line (1°C for the chilled water) on either side. This way the amount of more critical errors can be seen more clearly.

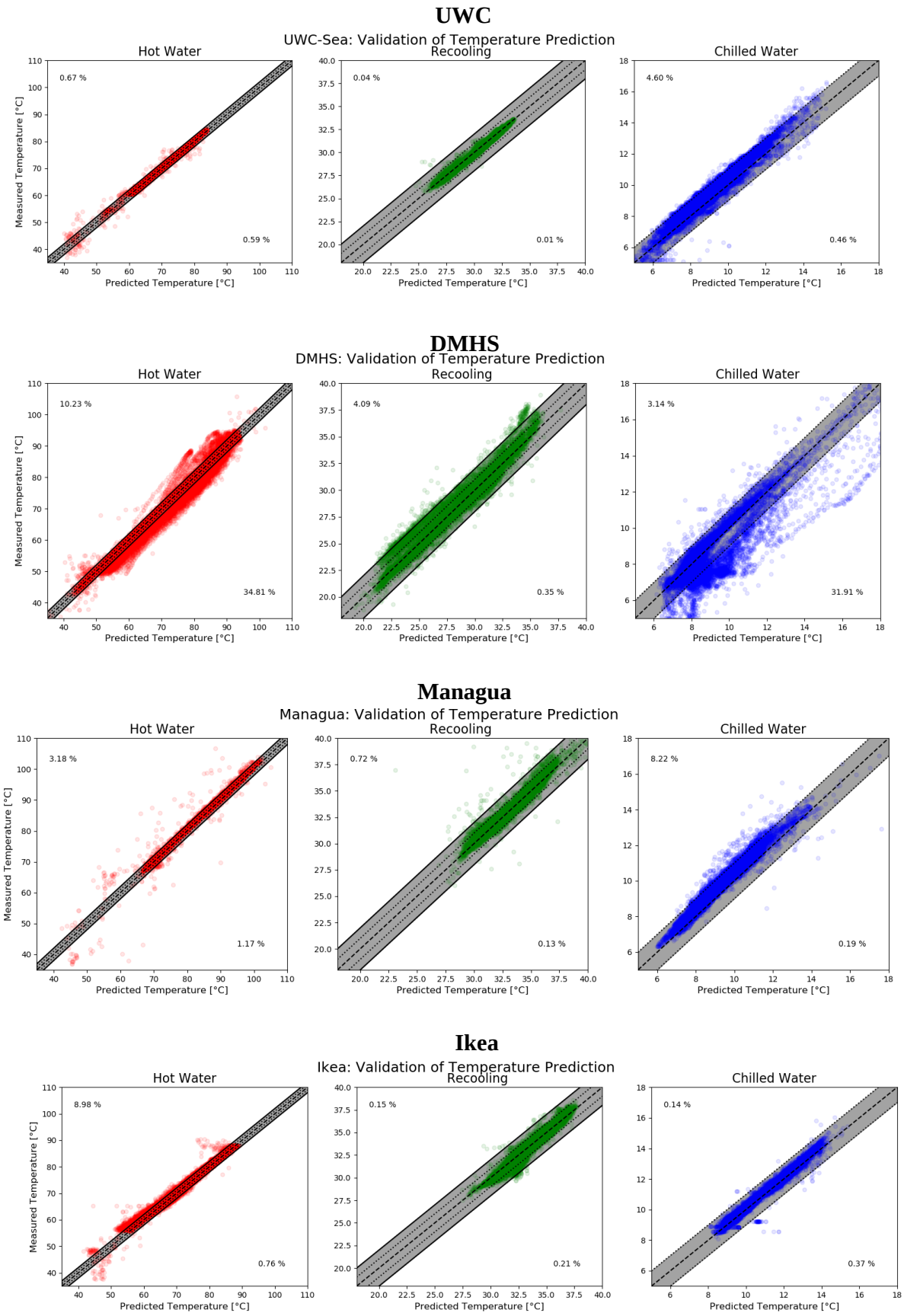

Fig.4: Comparison of measured and predicted data for each system and each output of the neural network with measured values on the y axis and predicted values on the x-axis.

For UWC very good results were obtained, with scores similar to the validation set (ref Tab.3 and Fig.3). Both the R^2 and the RMSE are within reasonable ranges with a R^2 of 94.45% and RMSE of lower than 0.63°C. The RMSE for the cooling water Temperature is especially well, as there is no speed control at the cooling water pump. In accordance to the scores, Fig.4 shows that the predicted temperatures at UWC are quite close to the measured ones. The diagram contains almost no outliers outside of the margins of 2°C and 1°C. The successful prediction can also be seen in Fig.5 showing that the ANN is also able to model sudden fluctuations at the chilled water side easily. In summary the ANN works very well in the case of UWC.

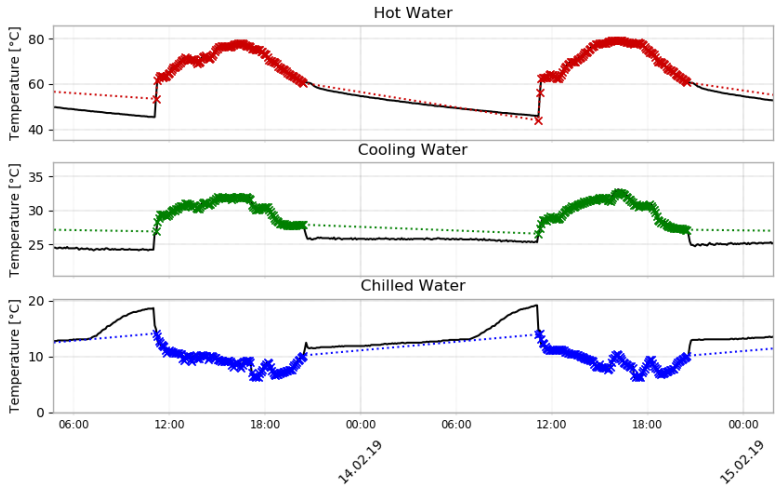

Fig.5: Comparison of measured and predicted data for UWC at each circuit. The coloured 'x' marker visualises the predicted values whereas the measured values are displayed as black lines.

In contrast, DMHSs result are bad: The R^2 score is noticeably smaller than at the validation in section 4.1 and the RMSE are very high, especially for the hot water and chilled water circuit. This can also be seen more clearly at Fig.4 where a lot of values are out of bounds.

The reason for this is a chiller service that was conducted at some time during the period of the test set. If the test-set gets subdivided into two parts, one containing the data of before the service was done and one set with data after the service was conducted, and the tests are run for both segments individually, the influence of the service can be seen more clearly. In fact, the ANN can predict the pre-service period quite accurately with a R^2 of 97,00% and RMSEs of 1.49 °C for the hot water temperature, 0.25°C for the cooling water temperature and 0.27°C chilled water temperature (see Tab.3 at the bottom). The results for the pre-service case can also be seen in Fig.6, where the comparison with Fig.4 shows that the values now are within acceptable ranges. In contrast, for the other set both the hot water and the chilled water get predicted very inaccurately (see Tab.3). Interestingly, this means that critical interventions can be detected by the use of the ANN. For modelling the post-service data, however, a new neural network would have to be trained with the new data.

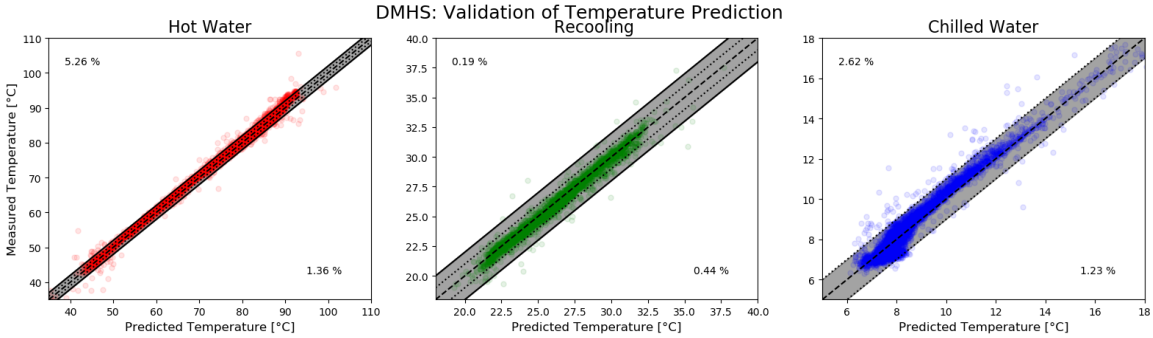

Fig.6: Comparison of measured and predicted temperatures at each circuit for DMHS if using data previous to the service conducted at the chiller.

Similar to DMHS, the R^2 score for Managua is below the score from the validation. Even tough the scores are all in appropriate ranges, this indicates problems in the data. Indeed, it can be seen in Fig.4 that the chilled water temperature predictions are shifted upwards the diagonal, that is, they are too high compared to the measured ones. This means that the chiller works worse than expected by the ANN-prediction during the test-period. To analyze this incidence further, the average daily error of the prediction of each circuit is shown for the test set in Fig.7. It can be seen that the error at the chilled water circuit is initially low for some time but then gradually gets worse over time. This indicates that something alters the performance of the chiller continuously during that period. Hence, the ANN is even able to detect subtle changes in the chiller operation and might be used to suggest service check-ups.

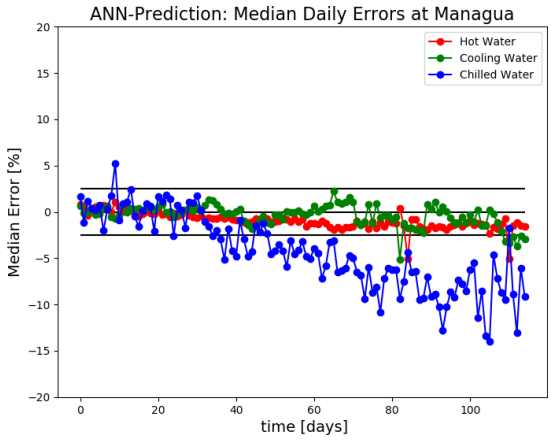

Fig.7: Median daily errors of the ANN-prediction in comparison to the measured values. Error margins of ±2.5% are visualized by black lines. The temperatures initially get predicted well until the chilled water gradually gets worse.

For Ikea the results shown in Tab.3 are very well, similar to UWC. As shown in Fig.4 the trained ANN-model is able to predict the outlet temperatures of the chiller very accurately. Only at the Hot Water circuit some of the predicted values are too low in comparison to the measured values for rather low temperatures of 55°C to 65°C. This is the case especially during start-up and shutdown of the chiller as can be seen paradigmatically in Fig.8. Nevertheless, the predictions are very accurate with a RMSE of only 1.84°C for the hot water side, 0.21°C for the cooling water and only 0.10°C for the chilled water side.

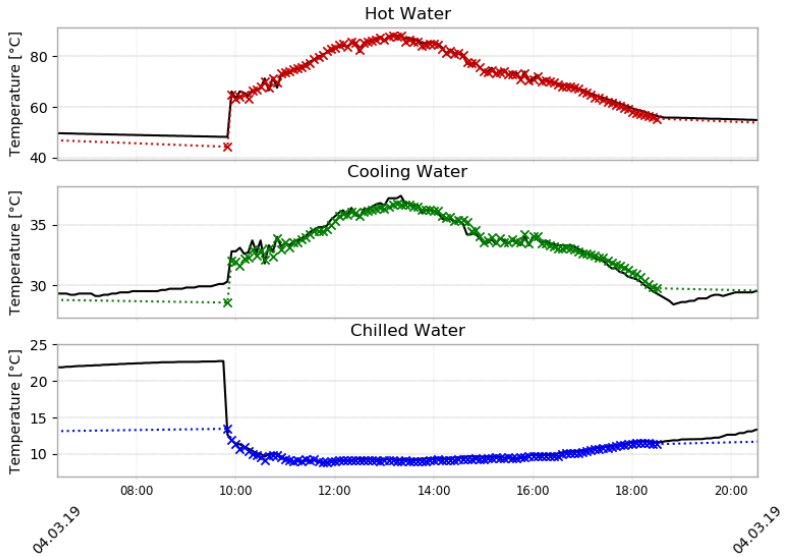

Fig.8: Comparison of measured and predicted data for Ikea for each circuit. The coloured 'x' marker visualises the predicted values whereas the measured values are displayed as black lines. The highest errors can be seen at the start-up of the chiller.

5. Conclusion

In this paper, the capabilities of artificial neuronal networks to predict the performance of absorption chillers at solar thermal systems were studied. The model derived in section 2 allows to introduce time delays and uses the inlet temperatures and the mass flows as input to predict the outlet temperatures of the chiller. The resulting model was applied to four of the currently largest solar thermal cooling systems worldwide, enabling to study the prediction ability of ANNs on systems in operation and with different climate conditions.

The results indicate that even quite simple architectures are sufficient for the prediction and optimal values for the time delay (40 Minutes) and the number of neurons (1 hidden layer with 25 neurons) were derived. The performance-results show very good agreement of the prediction and the measured values with RMSE of lower than 2.2°C for the hot water side, 0.80°C for the cooling water side and 0.41°C for the chilled water circuit at each system. As seen in Fig.4 and Fig.6, only few percent of the data is outside of the boundaries of 2°C for the hot water and cooling water and 1°C for the chilled water side. More clearly the timeseries in Fig.5 and Fig.8 show the capabilities of the network to correctly predict the outlet temperatures based on the input.

To sum up, the ANN-model is very successful on large-scale SAC systems, hence, showing high potentials for various applications. For example, the prediction might be used for fault detection, as the results for DMHS and Managua show (Fig.4, Fig.6, Fig.7). Plus, one could provide the ANN with artificial data and try to find the optimal parameters for the operation of the chiller. This would allow to analyze the system without running costly in-situ simulations. Finally, the results also indicate that the application of ANN on absorption heat pumps most likely would yield similar results and could be used in analog ways to optimize the operation of the system.

6. Acknowledgements

The results of this paper were obtained as preliminary results from the sBSc project, which is studying control strategies for BIG-Solar technologies extensively and is financed by the SFG and EFRE. The authors would thus like to thank all companies and institutions included in the sBSc project.

7. References

Buchinger, J., Holter, C., Blazek, H., 2012. Financing of large solar thermal systems for cooling and process heat. Energy Procedia 2012, Vol.30, 1372-1379. DOI: 10.1016/j.egypro.2012.11.151

Bishop, C.M., 2006. Pattern Recognition and Machine Learning. Springer, New York.

Frey, P., Fischer, S., Drück, H., 2014. Artificial Neural Network modelling of sorption chillers. Solar Energy, Vol.108, pp.525-537.

Lazrak, A., Boudehenn, F., Bonnot, S., Fraisse, G., Leconte, A., Papillon, P., Souyri, B., 2016. Development of a dynamic artificial neural network model of an absorption chiller and its experimental validation. Renewable Energy, Vol.86, pp.1009-1022.

Manohar, H.J., Saravanan, R.. Renganarayanan, S., 2006. Modelling of steam fired double effect vapour absorption chiller using neural network. Energy Conversion and Management, Vol.47(15), pp.2202-2210.

Nasruddin, M., Aisyah, N., Alhamid, M.I., Saha, B.B., Sholahudin, S., Lubis, A., 2019. Solar absorption chiller performance prediction based on the selection of principal component analysis. Case Studies in Thermal Engineering, Vol.13, p.100391.

OECD/IEA, 2018. The Future of Cooling - Opportunities for energy-efficient air conditioning. IEA Publishing, License: www.iea.org/t&c

Ohnewein, P., Schrammel, H., Tschopp, D., Krammer, S., Poier, H., Gerardts, B., Köstinger, A., Weinhappl, A., 2015. METHODIQA – Development of a quality assurance methodology for renewable heat systems based on intelligent operational monitoring. Energy Procedia 2016, Vol.91, 376-383. DOI: 10.1016/j.egypro.2016.06.285

Olsacher, N., Schnitzer, H., 2016. Solar Heating and Cooling for Tropical Countries Experiences, Chances, Hurdles. Proceedings of the International Conference 2016 ICENR - ILTER-EAP, pp.390-394.

Pedregosa, F., Varoquaux, G., Gramfort, A., Michel, V., Thirion, B., Grisel, O., Blondel, M., Prettenhofer, P., Weiss, R., Dubourg, V., Vanderplas, J., Passos, A., Cournapeau, D., Brucher, M., Perrot, M., Duchesnay, E., 2011.

Scikit-learn: Machine Learning in Python. Journal of Machine Learning Research, Vol.12, pp.2825-2830.

Pons, M., Anies, G., Boudehenn, F., Bourdoukan, P., Castaing-Lasvignottes, J., Evola, G., Le Denn, A., Le Pierrès, N., Marc, O., Mazet, N., Stitou, D., Lucas, F., 2012. Performance comparison of six solar-powered air-conditioners operated in five places. Energy, Vol.46(1), pp.471-483.

Rosiek, S., Batlles, F.J., 2010. Modelling a solar-assisted air-conditioning system installed in CIESOL building using an artificial neural network. Renewable Energy, Vol.35(12), pp.2894-2901.

Rosiek, S., Batlles, F.J., 2011. Performance study of solar-assisted air-conditioning system provided with storage tanks using artificial neural networks. International Journal of Refrigeration, Vol.34, pp.1446-1454.

Schubert, M., Holter, C., Luttenberger, J., 2011. Solar Cooling with Cooling Power Beyond One Megawatt - new Installations in Singapore and USA, in: OTTI 4th International Conference Solar Air-Conditioning, Larnaca, pp.269-271.

Schubert, M., Holter, C., Blazek, H., 2014. First operation months of world's most powerful solar cooling system in the USA at Desert Mountain High School (DMHS), Scottsdale, AZ. ISES Conference Proceedings 2014, 654-656. DOI: 10.18086/eurosun.2014.07.15

Xu, Z.Y., Wang, R.Z., 2017. Simulation of solar cooling system based on variable effect LiBr-water absorption chiller. Renewable Energy, Vol.113, 907-914.

8. Web-References

Weiss, W., Spörk-Dür, M., 2018. Solar Heat Worldwide. URL:https://www.iea-shc.org/Data/Sites/1/publications/Solar-Heat-Worldwide-2018.pdf, last accessed: 23.07.2019.

SOLID Website. Solar Cooling and hot water for Managua Hospital. URL: https://www.solid.at/en/references/solar-cooling, last accessed: 23.07.2019.

Technology Collaboration Programme on Heat Pumping Technologies (HPT TCP), 2018a. Flue gas condensation at the biomass cogeneration plant Klagenfurt-East. URL: https://heatpumpingtechnologies.org/annex47/wp-content/uploads/sites/54/2018/12/klagenfurt.pdf, last accessed: 16.08.2019.

Technology Collaboration Programme on Heat Pumping Technologies (HPT TCP), 2018b. BIGSOLAR – GRAZ. URL: https://heatpumpingtechnologies.org/annex47/wp-content/uploads/sites/54/2018/12/gaz-bigsolar.pdf, last accessed:16.08.2019.